

Delving Deep into Label Smoothing

Chang-Bin Zhang*, Peng-Tao Jiang*, Qibin Hou, Yunchao Wei, Qi Han, Zhen Li, and Ming-Ming Cheng

Abstract—Label smoothing is an effective regularization tool for deep neural networks (DNNs), which generates soft labels by applying a weighted average between the uniform distribution and the hard label. It is often used to reduce the overfitting problem of training DNNs and further improve classification performance. In this paper, we aim to investigate how to generate more reliable soft labels. We present an Online Label Smoothing (OLS) strategy, which generates soft labels based on the statistics of the model prediction for the target category. The proposed OLS constructs a more reasonable probability distribution between the target categories and non-target categories to supervise DNNs. Experiments demonstrate that based on the same classification models, the proposed approach can effectively improve the classification performance on CIFAR-100, ImageNet, and fine-grained datasets. Additionally, the proposed method can significantly improve the robustness of DNN models to noisy labels compared to current label smoothing approaches. The code will be made publicly available.

I. INTRODUCTION

DEEP Neural Networks (DNNs) [1], [2], [3], [4], [5], [6], [7] have achieved remarkable performance in image recognition [8], [9]. However, most DNNs tend to fall into over-confidence for training samples, greatly influencing their generalization ability to test samples. Recently, researchers have proposed many regularization approaches, including Label Smoothing [10], Bootstrap [11], CutOut [12], MixUp [13], DropBlock [14] and ShakeDrop [15], to conquer the overfitting problem to the distribution of the training set. These methods attempt to tackle this problem from the views of data augmentation [12], [13], model design [14], [15], or label transformation [10], [11]. Among them, label smoothing is a simple yet effective regularization tool operating on the labels.

Label smoothing (LS), aiming at providing regularization for a learnable classification model, is first proposed in [10]. Instead of merely leveraging the hard labels for training (Fig. 1(a)), Christian *et al.*[10] utilizes soft labels by taking an average between the hard labels and the uniform distribution over labels (Fig. 1(b)). Although such kind of soft labels can provide strong regularization and prevent the learned models from being over-confident, it treats the non-target categories equally by assigning them with fixed identical probability. For example, a ‘cat’ should be more like a ‘dog’ rather than an ‘automobile.’ Therefore, we argue that the assigned probabilities of non-target categories should highly consider their similarities to the category of the given image. Equally treating each non-target category could weaken the capability of label smoothing and limit the model performance.

It has been demonstrated in [16] that model predictive distributions provide a promising way to reveal the implicit relationships among different categories. Motivated by this knowledge, we propose a simple yet effective method to generate more reliable soft labels that consider the relationships among different categories to take the place of label smoothing. Specifically, we maintain a moving label distribution for each category, which can be updated during the training process. The maintained label distributions keep changing at each training epoch and are utilized to supervise DNNs until the model reaches convergence. Our method takes advantage of the statistics of the intermediate model predictions, which can better build the relationships between the target categories and the non-target ones. It can be observed from Fig. 1(c) that our method gives more confidence to the animal categories instead of those non-animal ones when the label is ‘cat.’

We conduct extensive experiments on CIFAR-100, ImageNet [9] and four fine-grained datasets [17], [18], [19], [20]. Our OLS can make consistent improvements over baselines. To be specific, directly applying OLS to ResNet-56 and ResNeXt29-2x64d yields 1.57% and 2.11% top-1 performance gains on CIFAR-100, respectively. For ImageNet, our OLS can bring 1.4% and 1.02% performance improvements to ResNet-50 and ResNet-101 [2], respectively. On four fine-grained datasets, OLS achieves an average 1.0% performance improvement over LS [10] on four different backbones, i.e., ResNet-50 [2], MobileNetv2 [6], EfficientNet-b7 [21] and SAN-15 [22]. The proposed OLS can be naturally employed to tackle noisy labels by reducing the overfitting to training sets. Additionally, OLS can be conveniently used in the training process of many models. We hope it can serve as an effective regularization tool to augment the training of classification models.

II. RELATED WORK

Regularization tools on labels. Training DNNs with hard labels (assigning 1 to the target category and 0 to the non-target ones) often results in over-confident models. Boosting labels is a straightforward yet effective way to alleviate the overfitting problem and improve the accuracy and robustness of DNNs. Bootstrapping [11] provided two options, Bootsoft and Boothard, which smoothed the hard labels using the predicted distribution and the predicted class, respectively. Xie *et al.* [23] randomly perturbed labels of some samples in a mini-batch to regularize the networks. To further prevent the training models from overfitting to some specific samples, Dubey *et al.* [24] added pairwise confusion to the output logits of samples belonging to different categories in training so that the models can learn slightly less discriminative features for specific samples. Li *et al.* [25] used two networks to embed the images and the labels in a latent space and regularize the

C.B. Zhang, P.T. Jiang, Q. Han, Z. Li and M.M. Cheng are with TKLNDST, CS, Nankai University. M.M. Cheng is the corresponding author (cmm@nankai.edu.cn). * denotes equal contribution.

Q. Hou is with the National University of Singapore.

Y. Wei is with the University of Technology Sydney.

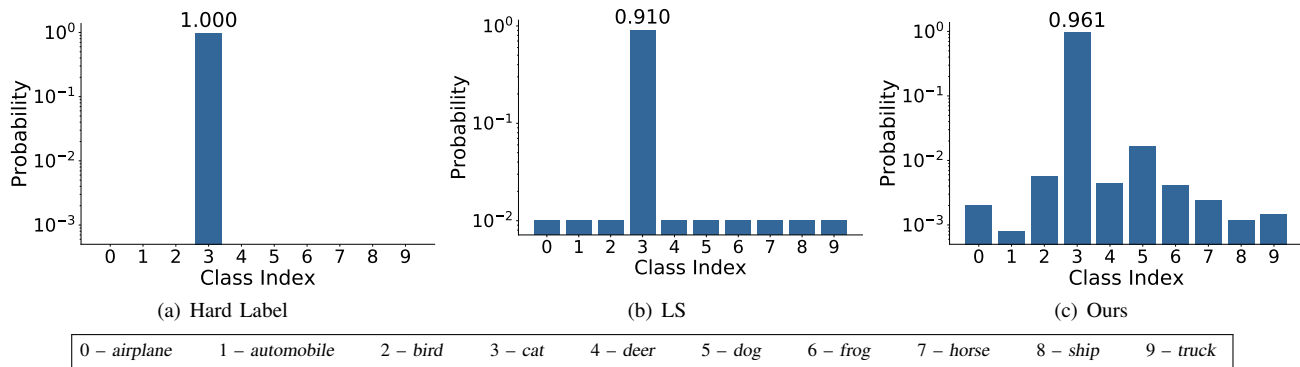


Fig. 1. Different kinds of label distributions on the CIFAR-10 dataset. The target category is ‘cat.’ We scale the y -axis using the \log function for visualization. (a) Original hard label. (b) Soft label generated by LS [10]. This soft label is a mixture of the hard label and uniform distribution. (c) Soft label generated by our OLS method during the training process of ResNet-29.

network via the distance between these embeddings. Christian *et al.* [10] leveraged soft labels for training, where the soft labels are generated by taking an average between the hard labels and the uniform distribution over labels. Our OLS also focuses on generating soft labels that can provide stable regularization for models. Unlike the mentioned approaches above, the soft labels generated by OLS take advantage of the statistical characteristics of model predictions of intermediate states.

Knowledge distillation. Knowledge distillation [16], [26], [27], is a popular way to compress models, which can significantly improve the performance of light-weight networks. Knowledge distillation has been widely used in many tasks [28], [29], [30]. It shows that DNNs can discover the similarities among different categories [16], [27] hidden in the predictions. Inspired by knowledge distillation, some works [31], [32], [27] utilized a self-distillation strategy to improve classification accuracy. Zhang *et al.* [31] distilled the knowledge from the deeper softmax layer to the shallower softmax layer. Xu *et al.* [32] encouraged the output of the augmented samples (using data augmentation methods) to be consistent with the original samples. Furlanello *et al.* [27] proposed to distill the knowledge of the teacher model to the student model with the same architecture. The student model obtained a higher accuracy than the teacher model. At the same time, Tommaso *et al.* [27] also verified the importance of the similarity between categories in the soft labels. Our work is inspired by knowledge distillation, aiming to find a reasonable similarity among categories.

Classification against noisy labels. Noisy labels in current datasets are inevitable due to the incorrect annotations by humans. To deal with this problem, many researchers explored solutions to this problem from both models [33], [34], data [35], [36] and training strategies [37], [38], [39]. A typical idea [40], [41], [42] is to weight different samples to reduce the influence of noisy samples on training. Ren *et al.* [40] verified each mini-batch on the clean validation set to adjust each sample’s weight in a mini-batch dynamically. MetaWeightNet [41] also exploited the clean validation set to learn the weights for samples by a multilayer perceptron (MLP). Moreover, some researchers solve this problem from the optimization perspective [43], [44]. Wang *et al.* [43] improved the robustness against noisy labels by replacing the normal cross-entropy function with the

symmetric cross-entropy function. Arazo *et al.* [45] observed that noisy samples often have higher losses than the clean ones during the early epochs of training. Based on this observation, they proposed to use the beta mixture model to represent clean samples and noisy samples and adopt this model to provide estimates of the actual class for noisy samples. Another kind of idea [46], [47] is to train the network with only the right labels. Although the proposed OLS is not specifically designed for noisy labels, the classification accuracy on noisy datasets is largely improved when training models with OLS. The performance gain owes to the ability of OLS to reduce the overfitting to training sets.

III. METHOD

A. Preliminaries

Given a dataset $\mathcal{D}_{\text{train}} = \{(\mathbf{x}_i, y_i)\}$ with K classes, where \mathbf{x}_i denotes the input image and y_i denotes the corresponding ground-truth label. For each sample (\mathbf{x}_i, y_i) , the DNN model predicts a probability $p(k|\mathbf{x}_i)$ for the class k using the softmax function. The distribution q of the hard label y_i can be denoted as $q(k = y_i|\mathbf{x}_i) = 1$ and $q(k \neq y_i|\mathbf{x}_i) = 0$. Then, the standard cross-entropy loss used in image classification for (\mathbf{x}_i, y_i) can be written as

$$L_{\text{hard}} = - \sum_{k=1}^K q(k|\mathbf{x}_i) \log p(k|\mathbf{x}_i) = - \log p(k = y_i|\mathbf{x}_i). \quad (1)$$

Instead of using hard labels for model training, LS [10] utilizes soft labels that are generated by exploiting a uniform distribution to smooth the distribution of the hard labels. Specifically, the probability of \mathbf{x}_i being class k in the soft label can be expressed as

$$q'(k|\mathbf{x}_i) = (1 - \varepsilon)q(k|\mathbf{x}_i) + \frac{\varepsilon}{K}, \quad (2)$$

where ε denotes the smoothing parameter that is usually set to 0.1 in practice. The assumption behind LS is that the confidence for the non-target categories is treated equally as shown in Fig. 1(b). Although combining the uniform distribution with the original hard label is useful for regularization, LS itself does not consider the genuine relationships among different

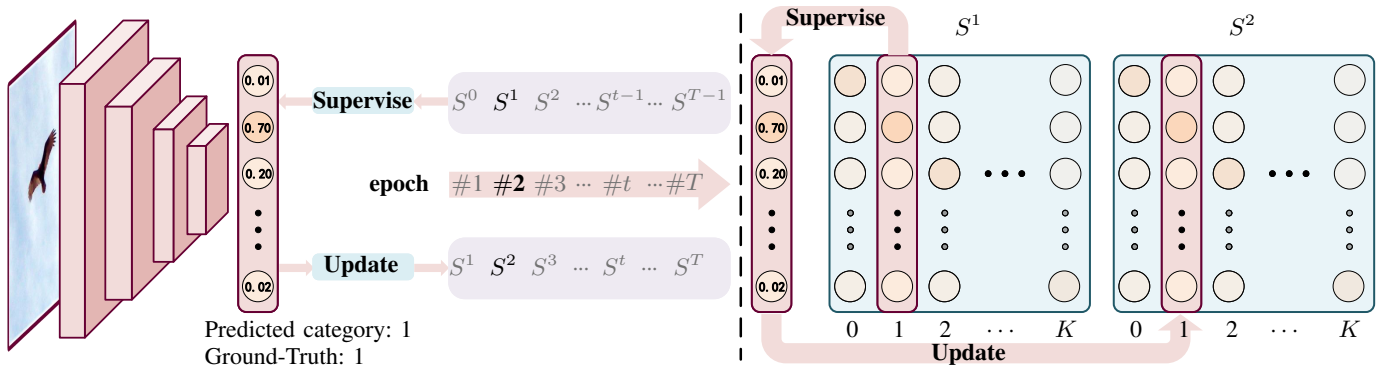


Fig. 2. The illustration of training DNN with our online label smoothing method. The left part of the figure shows the whole training process. We simply divided the training process into T phases according to the training epochs. K denotes the number of categories in datasets. We define each column of S^t to represent the soft label for a target category. At each epoch, we use the soft labels generated in the previous epoch to supervise the model, and meanwhile, we generate the soft labels for the next epoch. In the right, we show a detailed example of the training process in epoch#2. The generation of S^t is depicted in Sec. III.

categories [48]. We take this into account and present our online label smoothing method accordingly.

B. Online Label Smoothing

According to knowledge distillation, the similarity among categories can be effectively discovered from the model predictions [27], [16]. Motivated by this fact, unlike LS utilizing a static soft label, we propose to exploit model predictions to continuously update the soft labels during the training phase. Specifically, in the training process, we maintain a class-level soft label for each category. Given an input image x_i , if the classification is correct, the soft label corresponding to the target class y_i will be updated using the predicted probability $p(x_i)$. Then the updated soft labels will be subsequently utilized to supervise the model. The pipeline of our proposed method is shown in Fig. II.

Formally, let T denote the number of training epochs. We then define $S = \{S^0, S^1, \dots, S^t, \dots, S^{T-1}\}$ as the collection of the class-level soft labels at different training epochs. Here, S^t is a matrix with K rows and K columns, and each column in S^t corresponds to the soft label for one category. In the t_{th} training epoch, given a sample (x_i, y_i) , we use the soft label $S_{y_i}^{t-1}$ to form a temporary label distribution to supervise the model, where $S_{y_i}^{t-1}$ denotes the soft label for the target category y_i . The training loss of the model supervised by $S_{y_i}^{t-1}$ for (x_i, y_i) can be represented by

$$L_{soft} = - \sum_{k=1}^K S_{y_i, k}^{t-1} \cdot \log p(k|x_i). \quad (3)$$

It is possible that we directly use the above soft label to supervise the training model, but we find that the model is hard to converge due to the random parameter initialization at the beginning and the lack of the hard label. Thus, we utilize both the hard label and soft label as supervision to train the model. Now, the total training loss can be represented by

$$L = \alpha L_{hard} + (1 - \alpha) L_{soft}, \quad (4)$$

where α is used to balancing L_{hard} and L_{soft} .

Algorithm 1 The pipeline of the proposed OLS

Input: Dataset $\mathcal{D}_{train} = \{(x_i, y_i)\}$, model f_θ , training epochs T
Initialize: Soft label matrix $S^0 = \frac{1}{K} \mathbf{I}$, \mathbf{I} denotes unit matrix, K denotes the number of classes
for current epoch $t = 1$ **to** T **do**
 Initialize: $S^t = 0$
 for $iter = 1$ **to** $iterations$ **do**
 Sample a batch $\mathcal{B} \subset \mathcal{D}_{train}$, input to f_θ
 Obtain predicted probabilities $\{f(\theta, x_i), x_i \in \mathcal{B}\}$
 Compute loss by Eqn. (4), backward to update the parameter θ
 for $i = 1$ **to** $|\mathcal{B}|$ **do**
 Update $S_{y_i}^t \leftarrow S_{y_i}^t + f(\theta, x_i)$
 end for
 end for
 Normalize S^t at each column
end for

In the t_{th} training epoch, we also use the predicted probabilities of the input samples to update $S_{y_i}^t$, which will be utilized to supervise the model training in the $t + 1$ epoch. At the beginning of the t_{th} training epoch, we initialize the soft label S^t as a zero matrix. When an input sample (x_i, y_i) is correctly classified by the model, we utilize its predicted score $p(x_i)$ to update the y_i column in S_t , which can be formulated as

$$S_{y_i, k}^t = S_{y_i, k}^t + p(k|x_i), \quad (5)$$

where $k \in \{1, \dots, K\}$, indexing the soft label $S_{y_i}^t$. At the end of the t_{th} training epoch, we normalize the cumulative S^t column by column as represented by

$$S_{y_i, k}^t \leftarrow \frac{S_{y_i, k}^t}{\sum_{l=1}^K S_{y_i, l}^t}. \quad (6)$$

We can now obtain the normalized soft label S^t for all K categories, which will be used to supervise the model at the next training epoch. Notice that we cannot obtain the soft label at the first epoch. Thus, we use the uniform distribution to

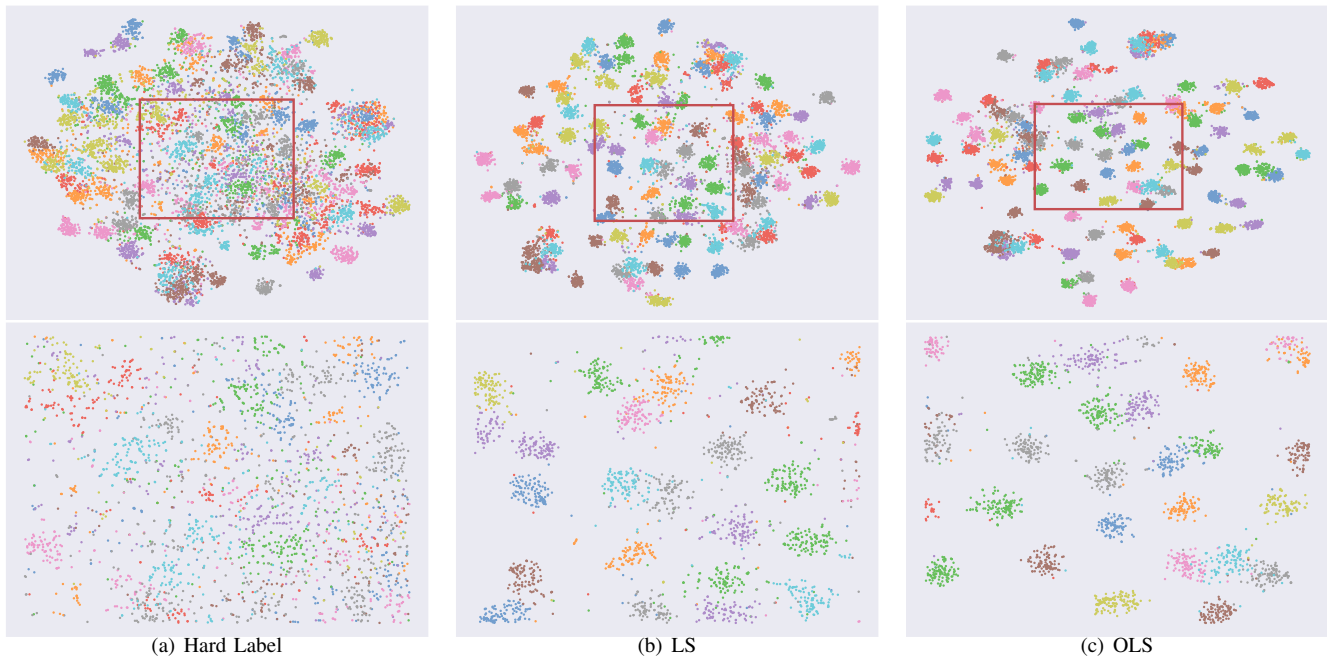


Fig. 3. Visualization of the penultimate layer representations of ResNet-56 on CIFAR-100 training set using t-SNE [49]. Note that we use the same color for every 10 classes. We visualize the representations of all 100 classes (**top**). We zoom the patch in red boxes for better visualization. (**bottom**).

initialize each column in S^0 . More details for the proposed approach are described in Algorithm 1.

a) *Discussion:* The soft label $S_{y_i,k}^{t-1}$ generated from the $t-1$ epoch can be denoted as

$$S_{y_i,k}^{t-1} = \frac{1}{N} \sum_{j=1}^N p^{t-1}(k|\mathbf{x}_j), \quad (7)$$

where N denotes the number of correctly predicted samples with label y_i . $p^{t-1}(k|\mathbf{x}_j)$ is the output probability of category k when input \mathbf{x}_j to the network at the $t-1$ epoch. Then Eqn. (3) can be rewritten as

$$\begin{aligned} L_{soft} &= - \sum_{k=1}^K \frac{1}{N} \sum_{j=1}^N p^{t-1}(k|\mathbf{x}_j) \cdot \log p(k|\mathbf{x}_i) \\ &= - \frac{1}{N} \sum_{j=1}^N \sum_{k=1}^K p^{t-1}(k|\mathbf{x}_j) \cdot \log p(k|\mathbf{x}_i). \end{aligned} \quad (8)$$

This equation indicates that all correctly classified samples \mathbf{x}_j will impose a constraint to the current sample \mathbf{x}_i . The constrain encourages the samples belonging to the same category to be much closer. To give a more intuitive explanation, we utilize t-SNE [49] to visualize the penultimate layer representations of ResNet-56 on CIFAR-100 trained with the hard label, LS, and OLS, respectively. Fig. 3 shows that our proposed method provides a more recognizable difference between representations of different classes and tighter intra-class representations.

Besides, our method does not have the problem of training divergence in the early stages of training. This is because we use a uniform distribution as the soft label in the first epoch of training, which is equivalent to the vanilla label smoothing. In the entire training process afterwards, we only accumulate

correct predictions, which guarantees the correctness of the generated soft labels.

IV. EXPERIMENTS

In Sec. IV-A, we first present and analyze the performance of our approach on CIFAR-100, ImageNet, and some fine-grained datasets. Then, we test the tolerance to symmetric noisy labels in Sec. IV-B and robustness to adversarial attacks in Sec. IV-C, respectively. In Sec. IV-D, we apply our OLS to object detection. Moreover, in Sec. IV-E, we conduct extensive ablation experiments to analyze the settings of our method. All the experiments are implemented based on PyTorch platform [50].

A. General Image Recognition

CIFAR Classification. First, we conduct experiments on CIFAR-100 dataset to compare our OLS with other related methods, including regularization methods on labels (Bootstrap [11], Disturb Label [23], Symmetric Cross Entropy [43], Label Smoothing [10] and Pairwise Confusion [24]) and self-knowledge distillation methods (Xu *et al.* [32] and BYOT [31]). For a fair comparison with them, we keep the same experimental setup for all methods. Specifically, we train all the models for 300 epochs with a batch size of 128. The learning rate is initially set to 0.1 and decays at the 150th and 225th epoch by a factor of 0.1, respectively. For other hyper-parameters in different methods, we keep their original settings. Additionally, for a fair comparison with BYOT [31] and Xu *et al.* [32], we remove the feature-level supervision in them and only use the class labels to supervise models.

Tab. I shows the classification results of each method based on different network architectures. It can be seen that our method significantly improves the classification performance

TABLE I

COMPARISON BETWEEN OUR METHOD AND THE STATE-OF-THE-ART APPROACHES. WE RUN EACH METHOD THREE TIMES ON CIFAR-100 AND COMPUTE THE MEAN AND STANDARD DEVIATION OF THE TOP-1 ERROR (%). BEST RESULTS ARE HIGHLIGHTED IN **BOLD**.

Method	ResNet-34	ResNet-50	ResNet-101	ResNeXt29-2x64d	ResNeXt29-32x4d
Hard Label	20.62 ± 0.21	21.21 ± 0.25	20.34 ± 0.40	20.92 ± 0.52	20.85 ± 0.17
Bootsoft [11]	21.65 ± 0.13	21.25 ± 0.67	20.37 ± 0.07	21.20 ± 0.13	20.86 ± 0.24
Boothard [11]	22.58 ± 0.02	20.81 ± 0.13	21.46 ± 0.22	21.00 ± 0.10	21.47 ± 0.59
Disturb Label [23]	20.91 ± 0.30	22.12 ± 0.51	20.99 ± 0.12	21.64 ± 0.24	21.69 ± 0.06
Symmetric Cross Entropy [43]	22.86 ± 0.08	22.12 ± 0.11	22.60 ± 0.64	23.07 ± 0.28	22.96 ± 0.09
LS [10]	20.94 ± 0.08	21.20 ± 0.25	20.12 ± 0.02	20.34 ± 0.24	19.56 ± 0.18
Pairwise Confusion [24]	22.91 ± 0.04	23.09 ± 0.53	22.73 ± 0.39	21.55 ± 0.11	21.74 ± 0.04
Xu <i>et al.</i> [32]	20.04 ± 0.11	22.05 ± 0.43	21.70 ± 0.77	22.81 ± 0.08	23.14 ± 0.04
OLS	22.6 ± 0.09	20.65 ± 0.14	19.66 ± 0.15	18.81 ± 0.45	18.79 ± 0.20
BYOT [31]	20.41 ± 0.10	19.20 ± 0.30	18.51 ± 0.49	19.69 ± 0.12	20.33 ± 0.19
BYOT [31] + OLS	19.44 ± 0.09	18.15 ± 0.21	18.14 ± 0.08	18.29 ± 0.20	19.25 ± 0.29

on both lightweight and complex models, which indicates its robustness to different networks. Since BYOT [31] is learned with deep supervision, it performs better on deeper models, like ResNet-50 and ResNet-101, than our method. However, our method can be easily plugged into BYOT [31] and achieves better results than BYOT on deeper models. In addition, comparing to LS [10], our method achieves stable improvement on different models. Especially, our method outperforms LS by about 1.5% on ResNeXt29-2x64d. We argue that the performance gain owes to the useful relationships among categories discovered by our soft labels. In Sec. IV-E, we will further analyze the importance of building relationships among categories.

ImageNet Classification. We also evaluate our method on a large-scale dataset, ImageNet. It contains 1K categories with a total of 1.2M training images and 50K validation images. Specifically, we use the SGD optimizer to train all the models for 250 epochs with a batch size of 256. The learning rate is initially set to 0.1 and decays at the 75th, 150th, and 225th epochs, respectively. We report the best performance of each method.

The classification performance on ImageNet dataset is shown in Tab. II. Applying our OLS to ResNet-50 achieves 22.28% Top-1 Error, which is better than the result with LS [10] by 0.54%. Additionally, ResNet-101 with our OLS can achieve 20.85% top-1 error, which improves ResNet-101 by 1.02% and ResNet-101 with LS by 0.42%, respectively. This demonstrates that our OLS still performs well on the large-scale dataset. Moreover, we explore the combination of our method with other strategies, i.e., data augmentation (CutOut [12]) and self-distillation (BYOT [31]). In Tab. II, we observe the combination with them brings extra performance gains to ResNet50 and ResNet101. Our OLS can be utilized as a plug-in regularization module, which is easy to be combined with other methods.

Fine-grained Classification. The fine-grained image classification task [51], [52], [53], [54] focuses on distinguishing subordinate categories within entry-level categories [24], [55], [56], [57], [58], [59]. We conduct experiments on four fine-grained image recognition datasets, including CUB-200-2011 [18], Flowers-102 [17], Cars [19] and Aircrafts [20], respectively. In Tab. III, we present the details of these datasets. For all experiments, we keep the same experimental setup.

TABLE II
CLASSIFICATION RESULTS ON IMAGENET.

Model	Top-1 Error(%)	Top-5 Error(%)
ResNet-50	23.68	7.05
ResNet-50 + Bootsoft [11]	23.49	6.85
ResNet-50 + Boothard [11]	23.85	7.07
ResNet-50 + LS [10]	22.82	6.66
ResNet-50 + CutOut [12]	22.93	6.66
ResNet-50 + Disturb Label [23]	23.59	6.90
ResNet-50 + BYOT [31]	23.04	6.51
ResNet-50 + OLS	22.28	6.39
ResNet-50 + CutOut [12] + OLS	21.98	6.18
ResNet-50 + BYOT [31] + OLS	21.88	6.27
ResNet-101	21.87	6.29
ResNet-101 + LS [10]	21.27	5.85
ResNet-101 + CutOut [12]	20.72	5.51
ResNet-101 + OLS	20.85	5.50
ResNet-101 + CutOut [9] + LS [10]	20.47	5.51
ResNet-101 + CutOut [9] + OLS	20.25	5.42

TABLE III
DETAILED INFORMATION OF THE FINE-GRAINED DATASETS.

Dataset	Categories	Training Samples	Test Samples
CUB-200-2011 [18]	200	5994	5794
Flowers-102 [17]	102	2040	6149
Cars [19]	196	8144	8041
Aircrafts [20]	90	6667	3333

Specifically, we use SGD as the optimizer and train all models for 100 epochs. The initial learning rate is set as 0.01 and it decays at the 45th epoch and 80th epoch, respectively. In Tab. IV, we report the average Top-1 Error(%) and Top-5 Error(%) of three runs. Experiment results demonstrate that OLS can also improve classification performance on the fine-grained datasets, which indicates our soft labels can benefit fine-grained category classification.

B. Tolerance to Noisy Labels

As demonstrated in [43], [60], there exist noisy (incorrect) labels in datasets, especially those obtained from webs. Due to the powerful fitting ability of DNNs, they can still fit noisy labels easily [61]. But this is harmful for the generalization of DNNs. To reduce such damage to the generalization ability of

TABLE IV

THE TOP-1 AND TOP-5 ERROR(%) OF DIFFERENT ARCHITECTURES ON FINE-GRAINED CLASSIFICATION DATASETS. ALL RESULTS ARE AVERAGED OVER THREE RUNS. THE Δ DENOTES THE AVERAGE IMPROVEMENT RELATIVE TO HARD LABEL ON ALL DATASETS AND BACKBONES.

Dataset	Backbones	Hard Label		LS		OLS	
		Top-1 Err(%)	Top-5 Err(%)	Top-1 Err(%)	Top-5 Err(%)	Top-1 Err(%)	Top-5 Err(%)
CUB-200-2011 [18]	ResNet-50 [2]	19.19 \pm 0.22	5.00 \pm 0.25	18.11 \pm 0.14	4.88 \pm 0.08	17.53 \pm 0.09	4.01 \pm 0.27
Flowers-102 [17]		9.31 \pm 0.19	2.43 \pm 0.14	7.58 \pm 0.07	1.93 \pm 0.03	7.14 \pm 0.14	1.55 \pm 0.07
Cars [19]		9.58 \pm 0.19	1.79 \pm 0.01	8.32 \pm 0.09	1.57 \pm 0.03	7.46 \pm 0.01	0.92 \pm 0.04
Aircrafts [20]		11.88 \pm 0.11	3.86 \pm 0.13	9.92 \pm 0.07	3.73 \pm 0.12	9.19 \pm 0.12	2.60 \pm 0.03
CUB-200-2011 [18]	MobileNetv2 [6]	22.24 \pm 0.33	6.61 \pm 0.21	21.33 \pm 0.29	7.05 \pm 0.09	20.05 \pm 0.11	5.08 \pm 0.12
Flowers-102 [17]		8.97 \pm 0.09	2.51 \pm 0.19	8.06 \pm 0.35	2.46 \pm 0.08	7.27 \pm 0.17	1.77 \pm 0.10
Cars [19]		11.71 \pm 0.13	2.29 \pm 0.12	10.17 \pm 0.07	2.33 \pm 0.05	9.25 \pm 0.05	1.33 \pm 0.02
Aircrafts [20]		13.16 \pm 0.33	4.15 \pm 0.19	12.05 \pm 0.29	4.08 \pm 0.17	10.53 \pm 0.25	2.96 \pm 0.15
CUB-200-2011 [18]	EfficientNet-b7 [21]	18.44 \pm 0.15	5.07 \pm 0.13	17.40 \pm 0.14	5.02 \pm 0.03	16.21 \pm 0.24	3.34 \pm 0.02
Flowers-102 [17]		9.50 \pm 0.07	2.04 \pm 0.07	9.42 \pm 0.34	2.34 \pm 0.13	8.16 \pm 0.12	1.63 \pm 0.15
Cars [19]		9.24 \pm 0.22	1.84 \pm 0.13	8.42 \pm 0.08	1.76 \pm 0.07	7.53 \pm 0.13	0.97 \pm 0.02
Aircrafts [20]		11.61 \pm 0.37	3.72 \pm 0.20	9.60 \pm 0.15	3.62 \pm 0.13	8.83 \pm 0.19	2.71 \pm 0.12
CUB-200-2011 [18]	SAN-15 [22]	19.05 \pm 0.39	5.37 \pm 0.25	17.54 \pm 0.30	5.43 \pm 0.19	17.28 \pm 0.14	4.08 \pm 0.07
Flowers-102 [17]		7.85 \pm 0.29	1.78 \pm 0.21	8.08 \pm 0.34	1.95 \pm 0.15	7.09 \pm 0.18	1.56 \pm 0.12
Cars [19]		9.23 \pm 0.07	1.78 \pm 0.02	8.55 \pm 0.15	1.87 \pm 0.04	7.55 \pm 0.14	1.08 \pm 0.07
Aircrafts [20]		11.31 \pm 0.13	3.79 \pm 0.08	9.96 \pm 0.09	3.45 \pm 0.14	9.43 \pm 0.08	2.95 \pm 0.09
Average Improvements (Δ)		0.00	0.00	1.11 \uparrow	0.02 \uparrow	2.00 \uparrow	0.96 \uparrow

TABLE V

THE CLASSIFICATION PERFORMANCE OF DIFFERENT METHODS UNDER DIFFERENT NOISY RATES. WE RUN EACH METHOD THREE TIMES UNDER DIFFERENT NOISY RATES AND COMPUTE THE MEAN AND STANDARD DEVIATION OF THE TOP-1 ERROR(%). THE BEST TWO RESULTS ARE IN **BOLD**.

Method/Noise Rate	0%	20%	40%	60%	80%
Hard Label	26.81 \pm 0.36	37.75 \pm 0.50	47.07 \pm 1.08	62.06 \pm 0.62	81.56 \pm 0.42
Bootsort [11]	27.28 \pm 0.35	37.99 \pm 0.43	46.96 \pm 0.33	63.76 \pm 0.85	80.32 \pm 0.33
Boothard [11]	26.02 \pm 0.22	36.21 \pm 0.29	42.73 \pm 0.16	54.95 \pm 2.20	81.20 \pm 1.26
Symmetric Cross Entropy [43]	28.97 \pm 0.31	38.40 \pm 0.12	46.97 \pm 0.65	62.13 \pm 0.55	82.66 \pm 0.10
Ren <i>et al.</i> [40]	38.38 \pm 0.35	43.74 \pm 1.21	49.83 \pm 0.53	57.65 \pm 0.98	73.04 \pm 0.15
MetaWeightNet [41]	29.51 \pm 0.51	35.06 \pm 0.48	43.58 \pm 0.93	56.15 \pm 0.60	87.25 \pm 0.22
Arazo <i>et al.</i> [45]	33.80 \pm 0.10	33.91 \pm 0.38	40.87 \pm 1.49	52.91 \pm 1.81	83.92 \pm 0.19
LS [10]	26.37 \pm 0.41	35.48 \pm 0.61	43.99 \pm 1.04	59.51 \pm 0.80	80.36 \pm 0.90
OLS	25.24 \pm 0.18	32.67 \pm 0.14	38.86 \pm 0.13	50.04 \pm 0.14	78.22 \pm 1.01

DNNs, researchers have proposed many methods, including weighting the samples [40], [41] and inferring the real labels of the noisy samples [11], [45]. We notice that our method can improve the performance of DNNs on noisy labels by reducing the fitting to noisy samples. We conduct experiments on CIFAR-100 to verify the regularization capability of our method on noisy data.

We follow the same experimental settings as in [43], [45]. We randomly select a certain number of samples according to the noisy rate and flip the labels of these samples to the wrong labels uniformly (symmetric noise) before training. Since both Ren *et al.* [40] and MetaWeightNet [41] need to split a part of the clean validation set from the training set, we keep their default optimal number of samples in the validation set.

In Tab. V, we report the classification results based on the ResNet-56 model when the noisy rate is set to {0%, 20%, 40%, 60%, 80%}, respectively. It can be seen that our method achieves comparable results with those methods [43], [40], [41], [45] that are specifically designed for noisy labels. Comparing with LS, our method achieves stable improvement under different noisy rates. We also visualize training and test errors during the training process. As shown

in Fig. 4, our method achieves higher training errors than models trained with hard labels and LS. However, our method has lower test errors. This demonstrates that our method can effectively reduce the overfitting to noisy samples.

C. Robustness to Adversarial Attacks

We evaluate the robustness of the models trained by different methods against adversarial attack algorithms on CIFAR-10 and ImageNet, respectively. We use the Fast Gradient Sign Method (FGSM) [62] and Projected Gradient Descent (PGD) [63] to generate adversarial samples. For FGSM, we keep its default setup. Therefore, the ℓ_∞ bound is set to 8 for all methods. For PGD, we apply the same experimental setup as in [64] except that we increase the iteration times to 20, which is enough to get better attack effects.

In Tab. VI, we have reported the Top-1 Error after the adversarial attack from the FGSM and PGD algorithms on the CIFAR-10 dataset. After the FGSM and PGD attack, the models trained with our method keep the lowest Top-1 Error rate. We can see that the models trained with our OLS algorithm are much more robust to the adversarial attack than those trained with other methods. Moreover, we apply the same experiments

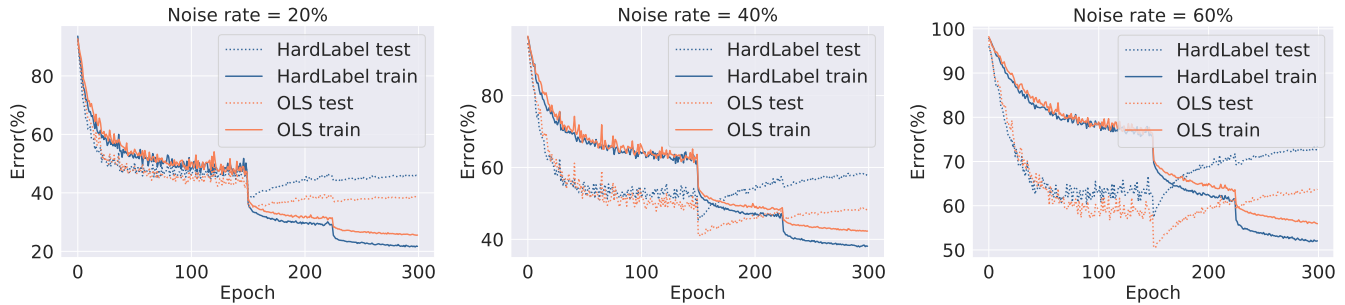


Fig. 4. We display the training error and test error under different noise rates (20%, 40%, 60%).

TABLE VI

ROBUSTNESS TO ADVERSARIAL ATTACK ON CIFAR-10. WE USE FGSM AND PGD ALGORITHMS TO ATTACK RESNET-29 TRAINED ON CIFAR-10, RESPECTIVELY. WE SET THE ITERATION TIMES OF PGD ATTACK ALGORITHM AS 20.

Method	ResNet-29	+ FGSM	+ PGD
	Top-1 Err(%)	Top-1 Err(%)	Top-1 Err(%)
Hard Label	7.18	82.46	93.18
Bootssoft [11]	6.91	79.83	92.57
Boothard [11]	7.73	82.68	90.01
Symmetric Cross Entropy [43]	8.66	77.68	93.96
LS [10]	6.81	79.48	87.32
OLS	6.46	60.39	76.29

TABLE VII

TOP-1 AND TOP-5 ERROR(%) OF RESNET-50 ON IMAGENET AFTER THE ADVERSARIAL ATTACK. FOR TWO ADVERSARIAL ATTACK ALGORITHMS, FGSM AND PGD, WE KEEP THEIR DEFAULT SETTING. WE SET THE ITERATION TIMES OF PGD ATTACK ALGORITHM AS 20.

ResNet-50	+ FGSM		+ PGD	
	Top-1 Err(%)	Top-5 Err(%)	Top-1 Err(%)	Top-5 Err(%)
Hard Label	91.07	66.21	94.93	31.82
Bootssoft [11]	91.29	67.29	94.56	31.07
LS [10]	74.44	50.63	80.31	24.46
OLS	75.79	48.13	74.43	22.14

TABLE VIII

OBJECT DETECTION RESULTS. WE TRAIN YOLO [65] ON PASCAL VOC DATASET.

Method	Hard Label	LS [10]	OLS
mAP (%)	81.6	82.3	82.7

on ImageNet, as shown in Tab. VII. Compared with the hard label, OLS achieves an average 17.9% gain in terms of Top-1 Error and an average 13.9% gain in terms of Top-5 Error. Our method can also outperform LS [10] by 2.3% and by 2.4% on Top-1 Error and Top-5 Error, respectively. We argue that the soft labels generated in our algorithm contain similarities between categories, making the distances of the embedding of samples in the same class closer. Experiments show that OLS can effectively improve the robustness of the model to adversarial examples.

D. Object Detection

Our OLS can be easily applied to the object detection framework [66], [67], [68], [69], [70]. We select YOLO [65]

as our basic detector. We train the detector on the popular PASCAL VOC dataset [71]. As shown in Tab. VIII, when YOLO is equipped with our OLS, it obtains a 1.1% gain over the hard label and a 0.4% gain over LS in terms of mean average precision (mAP), indicating OLS has stronger regularization ability than LS on the object detection.

Implement details. We use MobileNetv2 [6] as the backbone of YOLO [65]. We regard the combination of the training set and validation set from PASCAL VOC 2012 and PASCAL VOC 2007 as the training set. And we test the model on the PASCAL VOC 2007 test set. During training, we use standard training strategies, including warming up, multi-scale training, random crop, etc. We train the model for 120 epochs using SGD optimizer with an initial learning rate 0.0001 and cosine learning rate decay schedule. During tests, we also use multi-scale inference.

E. Ablation Study

In this subsection, we first conduct experiments to study the hyper-parameters in our method. Then we analyze the relationships among categories indicated by our soft labels. Besides, we also present a variant of OLS. Finally, we present the calibration effect of our method. All the experiments are conducted on the CIFAR dataset.

Impact of Hyper-parameters. We first analyze the hyper-parameter α in Eqn. (4) using ResNet-29. Unlike previous experiments that directly set α to 0.5, we enumerate possible values with $\alpha \in \{0.1, 0.2, \dots, 1.0\}$. We plot the experiment results as shown in Fig. 5(a). It can be seen that the model achieves the lowest top-1 error when α is set to 0.5. Since the model lacks guidelines for the correct category, we observe that when α is set to 0, the model is hard to convergent. When α changes from 0.1 to 0.5, the error rate gradually decreases. This fact suggests that the model still needs the correct category information provided by the original hard labels.

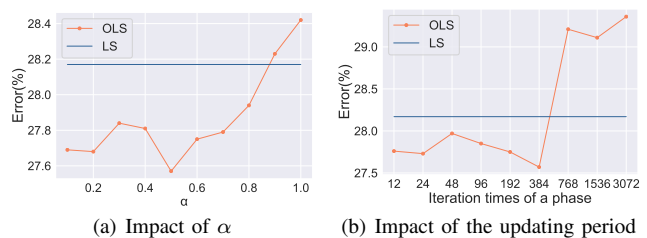


Fig. 5. Impact of hyper-parameters. The Top-1 Error of different α and updating period.

TABLE IX
TOP-1 ERROR(%) AND EXPECTED CALIBRATION ERROR(ECE) ON CIFAR-100. LOWER IS BETTER.

Method	ResNet-56		ResNet-74		ResNet-110	
	Top-1 Error(%)	ECE	Top-1 Error(%)	ECE	Top-1 Error(%)	ECE
Hard Label	26.81 \pm 0.36	11.37 \pm 0.53	25.86 \pm 0.19	12.70 \pm 0.76	25.54 \pm 0.44	13.14 \pm 1.16
LS [10]	26.37 \pm 0.41	3.35 \pm 0.86	25.90 \pm 0.31	2.37 \pm 0.94	25.14 \pm 0.31	2.32 \pm 1.03
OLS	25.24 \pm 0.18	2.85 \pm 1.44	24.89 \pm 0.08	1.81 \pm 0.85	23.86 \pm 0.27	2.05 \pm 0.68

Moreover, we also conduct experiments to study the impact of the updating period for the soft label matrix S in the training process. In the previous experiments in Sec. IV-A, we set the updating period to one epoch. As shown in Fig. 5(b), we evaluate our approach with different updating periods (iteration times $\in \{12, 24, 48, \dots, 1536, 3072\}$). The best performance is obtained when the updating period is set to one epoch. We observe that the classification performance is very close when the updating period is less than one epoch (1 epoch is approximately 384 iterations). However, when the updating period is longer than one training epoch, the performance decreases sharply. We analyze that with the training of the network, the predictions become better and better. When using more iterations to update soft labels, the relationships indicated by the early predictions will be very different from that of late ones. The early predictions become out of date for current training.

Importance of relationships among categories. We argue that classification models can benefit from soft labels that contain the knowledge of relationships among different categories. Specifically, we utilize a human uncertainty dataset [64] called CIFAR-10H to verify the reliability of the relationships among different categories. CIFAR-10H captures the full distribution of the labels by collecting votes from more than 50 people for each sample in the CIFAR-10 test set. The human uncertainty labels can be regarded as a kind of soft label that considers the similarities among different categories. They find that models trained on the human uncertainty labels will have better accuracy and generalization than those trained on hard labels. To explore the rationality of relationships among categories found by our approach, we use KL divergence to measure the difference between the predicted probability distribution of the model and the human uncertainty distribution on CIFAR-10H.

TABLE X

MULTIPLE EVALUATION RESULTS OF THE MODEL. WE FIRST TRAIN RESNET-29 WITH DIFFERENT METHODS ON CIFAR-10. WE USE THE AVERAGE KL DIVERGENCE TO MEASURE THE DIFFERENCE BETWEEN THE PREDICTION DISTRIBUTION OF THE MODELS AND HUMAN UNCERTAINTY ON CIFAR-10H TEST SET.

Method	CIFAR-10 Top-1 Err(%)	CIFAR-10H KL Divergence
Hard Label	7.18	0.2974
Bootsoft [11]	6.91	0.3247
Boothard [11]	7.73	0.3188
Symmetric Cross Entropy [43]	8.66	0.5563
LS [10]	6.81	0.1866
OLS	6.46	0.1399

For a fair comparison, we only consider the correctly

predicted samples by each model, when computing the KL Divergence on CIFAR-10H. As shown in Table X, we list the average KL divergence of different methods on CIFAR-10H [64] and Top-1 Error(%) on CIFAR-10. The results show that the prediction distribution of the model trained by our method is closer to that of humans. Also, this indicates that the model trained by our approach finds more reasonable and correct relationships among categories.

Sample-level soft labels. To verify the effectiveness of the statistical characteristics of accumulating model predictions, we use the predicted distribution of a single sample (denoted as OLS-Single for short) to regularize the training process. To be specific, for each training sample, we randomly select another training sample with the same category. We then acquire the randomly selected training sample’s predictive distribution and utilize this distribution as the soft label to serve as supervision for the current training sample. Based on the ResNet-56, OLS (25.24 \pm 0.18) outperforms OLS-Single (26.18 \pm 0.30) by about 1%. This result demonstrates that the accumulation of the predictions from different samples can well explore the relationships among categories.

Calibration effect. The confidence calibration is proposed in [72], which is used to measure the degree of overfitting of the model to the training set. We use the Expected Calibration Error (ECE) [72] to measure the calibration ability of OLS. In Tab. IX, we report the Top-1 Error(%) and ECE on several models, which denotes our method can calibrate neural networks. Experimental results show that our method achieves a lower Top-1 Error than LS by an average of 1.14%. Meanwhile, our method also achieves lower ECE values on three different depth models. This indicates that the proposed method can more effectively prevent over-confident predictions and show better calibration capability.

V. CONCLUSION

In this paper, we propose an online label smoothing method. We utilize the statistics of the intermediate model predictions to generate soft labels, which are subsequently used to supervise the model. Our soft labels considering the relationships among categories are effective in preventing the overfitting problem of DNNs to the training set. We evaluate our OLS on CIFAR, ImageNet and four fine-grained datasets, respectively. On CIFAR-100, ResNeXt-2x64d trained with our OLS achieves 18.81% Top-1 Error, which brings an 2.11% performance gain. On ImageNet dataset, our OLS brings 1.4% and 1.02% performance gains to ResNet-50 and ResNet-101, respectively. On four fine-grained datasets, OLS outperforms the hard label by 2% in terms of Top-1 Error.

REFERENCES

- [1] K. Simonyan and A. Zisserman, "Very deep convolutional networks for large-scale image recognition," in *Int. Conf. Learn. Represent.*, 2015.
- [2] K. He, X. Zhang, S. Ren, and J. Sun, "Deep residual learning for image recognition," in *IEEE Conf. Comput. Vis. Pattern Recog.*, 2016, pp. 770–778.
- [3] G. Huang, Z. Liu, L. Van Der Maaten, and K. Q. Weinberger, "Densely connected convolutional networks," in *IEEE Conf. Comput. Vis. Pattern Recog.*, 2017, pp. 4700–4708.
- [4] S. Xie, R. Girshick, P. Dollár, Z. Tu, and K. He, "Aggregated residual transformations for deep neural networks," in *IEEE Conf. Comput. Vis. Pattern Recog.*, 2017, pp. 1492–1500.
- [5] J. Hu, L. Shen, and G. Sun, "Squeeze-and-excitation networks," in *IEEE Conf. Comput. Vis. Pattern Recog.*, 2018, pp. 7132–7141.
- [6] M. Sandler, A. G. Howard, M. Zhu, A. Zhmoginov, and L. Chen, "Mobilenetv2: Inverted residuals and linear bottlenecks," in *IEEE Conf. Comput. Vis. Pattern Recog.*, 2018, pp. 4510–4520.
- [7] S.-H. Gao, M.-M. Cheng, K. Zhao, X.-Y. Zhang, M.-H. Yang, and P. Torr, "Res2net: A new multi-scale backbone architecture," *IEEE Trans. Pattern Anal. Mach. Intell.*, 2020.
- [8] A. Krizhevsky, "Learning multiple layers of features from tiny images," University of Toronto, Tech. Rep., 2009.
- [9] J. Deng, W. Dong, R. Socher, L.-J. Li, K. Li, and L. Fei-Fei, "Imagenet: A large-scale hierarchical image database," in *IEEE Conf. Comput. Vis. Pattern Recog.*, 2009, pp. 248–255.
- [10] C. Szegedy, V. Vanhoucke, S. Ioffe, J. Shlens, and Z. Wojna, "Rethinking the inception architecture for computer vision," in *IEEE Conf. Comput. Vis. Pattern Recog.*, 2016, pp. 2818–2826.
- [11] S. E. Reed, H. Lee, D. Anguelov, C. Szegedy, D. Erhan, and A. Rabinovich, "Training deep neural networks on noisy labels with bootstrapping," in *Int. Conf. Learn. Represent. Worksh.*, 2015.
- [12] T. DeVries and G. W. Taylor, "Improved regularization of convolutional neural networks with cutout," *arXiv preprint arXiv:1708.04552*, 2017.
- [13] H. Zhang, M. Cisse, Y. N. Dauphin, and D. Lopez-Paz, "mixup: Beyond empirical risk minimization," in *Int. Conf. Learn. Represent.*, 2018.
- [14] G. Ghiasi, T.-Y. Lin, and Q. V. Le, "Dropblock: A regularization method for convolutional networks," in *Adv. Neural Inform. Process. Syst.*, 2018, pp. 10727–10737.
- [15] Y. Yamada, M. Iwamura, T. Akiba, and K. Kise, "Shakedrop regularization for deep residual learning," *IEEE Access*, pp. 186 126–186 136, 2019.
- [16] G. Hinton, O. Vinyals, and J. Dean, "Distilling the knowledge in a neural network," in *Adv. Neural Inform. Process. Syst. Worksh.*, 2015.
- [17] M.-E. Nilsback and A. Zisserman, "Automated flower classification over a large number of classes," in *2008 Sixth Indian Conference on Computer Vision, Graphics & Image Processing*, 2008, pp. 722–729.
- [18] C. Wah, S. Branson, P. Welinder, P. Perona, and S. Belongie, "The Caltech-UCSD Birds-200-2011 Dataset," California Institute of Technology, Tech. Rep. CNS-TR-2011-001, 2011.
- [19] J. Krause, M. Stark, J. Deng, and L. Fei-Fei, "3d object representations for fine-grained categorization," in *Int. Conf. Comput. Vis. Worksh.*, 2013, pp. 554–561.
- [20] S. Maji, E. Rahtu, J. Kannala, M. Blaschko, and A. Vedaldi, "Fine-grained visual classification of aircraft," *arXiv preprint arXiv:1306.5151*, 2013.
- [21] M. Tan and Q. V. Le, "Efficientnet: Rethinking model scaling for convolutional neural networks," in *International Conference on Machine Learning*, vol. 97, 2019, pp. 6105–6114.
- [22] H. Zhao, J. Jia, and V. Koltun, "Exploring self-attention for image recognition," in *IEEE Conf. Comput. Vis. Pattern Recog.*, 2020, pp. 10 076–10 085.
- [23] L. Xie, J. Wang, Z. Wei, M. Wang, and Q. Tian, "Disturblabel: Regularizing cnn on the loss layer," in *IEEE Conf. Comput. Vis. Pattern Recog.*, 2016.
- [24] A. Dubey, O. Gupta, P. Guo, R. Raskar, R. Farrell, and N. Naik, "Pairwise confusion for fine-grained visual classification," in *Eur. Conf. Comput. Vis.*, 2018, pp. 70–86.
- [25] C. Li, C. Liu, L. Duan, P. Gao, and K. Zheng, "Reconstruction regularized deep metric learning for multi-label image classification," *IEEE Transactions on Neural Networks and Learning Systems*, vol. 31, no. 7, pp. 2294–2303, 2020.
- [26] N. Passalis and A. Tefas, "Unsupervised knowledge transfer using similarity embeddings," *IEEE Transactions on Neural Networks and Learning Systems*, vol. 30, no. 3, pp. 946–950, 2019.
- [27] T. Furlanello, Z. C. Lipton, M. Tschannen, L. Itti, and A. Anandkumar, "Born-again neural networks," in *International Conference on Machine Learning*, 2018, pp. 1602–1611.
- [28] S. Ge, Z. Luo, C. Zhang, Y. Hua, and D. Tao, "Distilling channels for efficient deep tracking," *IEEE Trans. Image Process.*, vol. 29, pp. 2610–2621, 2020.
- [29] N. Wang, W. Zhou, Y. Song, C. Ma, and H. Li, "Real-time correlation tracking via joint model compression and transfer," *IEEE Trans. Image Process.*, vol. 29, pp. 6123–6135, 2020.
- [30] S. Ge, S. Zhao, C. Li, and J. Li, "Low-resolution face recognition in the wild via selective knowledge distillation," *IEEE Trans. Image Process.*, vol. 28, no. 4, pp. 2051–2062, 2019.
- [31] L. Zhang, J. Song, A. Gao, J. Chen, C. Bao, and K. Ma, "Be your own teacher: Improve the performance of convolutional neural networks via self distillation," in *Int. Conf. Comput. Vis.*, 2019.
- [32] T.-B. Xu and C.-L. Liu, "Data-distortion guided self-distillation for deep neural networks," in *The National Conference on Artificial Intelligence (AAAI)*, 2019, pp. 5565–5572.
- [33] J. Yao, J. Wang, I. W. Tsang, Y. Zhang, J. Sun, C. Zhang, and R. Zhang, "Deep learning from noisy image labels with quality embedding," *IEEE Trans. Image Process.*, vol. 28, no. 4, pp. 1909–1922, 2019.
- [34] J. S. Duncan and T. Birkholzer, "Reinforcement of linear structure using parametrized relaxation labeling," *IEEE Trans. Pattern Anal. Mach. Intell.*, vol. 14, no. 5, pp. 502–515, 1992.
- [35] R. Wang, T. Liu, and D. Tao, "Multiclass learning with partially corrupted labels," *IEEE Transactions on Neural Networks and Learning Systems*, vol. 29, no. 6, pp. 2568–2580, 2018.
- [36] Y. Wei, C. Gong, S. Chen, T. Liu, J. Yang, and D. Tao, "Harnessing side information for classification under label noise," *IEEE Transactions on Neural Networks and Learning Systems*, vol. 31, no. 9, pp. 3178–3192, 2020.
- [37] B. Han, I. W. Tsang, L. Chen, C. P. Yu, and S. Fung, "Progressive stochastic learning for noisy labels," *IEEE Transactions on Neural Networks and Learning Systems*, vol. 29, no. 10, pp. 5136–5148, 2018.
- [38] D. Tanaka, D. Ikami, T. Yamasaki, and K. Aizawa, "Joint optimization framework for learning with noisy labels," in *IEEE Conf. Comput. Vis. Pattern Recog.*, 2018, pp. 5552–5560.
- [39] J. Han, P. Luo, and X. Wang, "Deep self-learning from noisy labels," in *Int. Conf. Comput. Vis.*, 2019, pp. 5137–5146.
- [40] M. Ren, W. Zeng, B. Yang, and R. Urtasun, "Learning to reweight examples for robust deep learning," in *International Conference on Machine Learning*, 2018, pp. 4334–4343.
- [41] J. Shu, Q. Xie, L. Yi, Q. Zhao, S. Zhou, Z. Xu, and D. Meng, "Meta-weight-net: Learning an explicit mapping for sample weighting," in *Adv. Neural Inform. Process. Syst.*, 2019, pp. 1919–1930.
- [42] T. Liu and D. Tao, "Classification with noisy labels by importance reweighting," *IEEE Trans. Pattern Anal. Mach. Intell.*, vol. 38, no. 3, pp. 447–461, 2015.
- [43] Y. Wang, X. Ma, Z. Chen, Y. Luo, J. Yi, and J. Bailey, "Symmetric cross entropy for robust learning with noisy labels," in *Int. Conf. Comput. Vis.*, 2019, pp. 322–330.
- [44] R. Tanno, A. Saeedi, S. Sankaranarayanan, D. C. Alexander, and N. Silberman, "Learning from noisy labels by regularized estimation of annotator confusion," in *IEEE Conf. Comput. Vis. Pattern Recog.*, 2019, pp. 11 236–11 245.
- [45] E. Arazo, D. Ortego, P. Albert, N. O'Connor, and K. McGuinness, "Unsupervised label noise modeling and loss correction," in *International Conference on Machine Learning*, 2019, pp. 312–321.
- [46] J. Zhang, V. S. Sheng, T. Li, and X. Wu, "Improving crowdsourced label quality using noise correction," *IEEE Transactions on Neural Networks and Learning Systems*, vol. 29, no. 5, pp. 1675–1688, 2018.
- [47] M. Fang, T. Zhou, J. Yin, Y. Wang, and D. Tao, "Data subset selection with imperfect multiple labels," *IEEE Transactions on Neural Networks and Learning Systems*, vol. 30, no. 7, pp. 2212–2221, 2019.
- [48] R. Müller, S. Kornblith, and G. E. Hinton, "When does label smoothing help?" in *Adv. Neural Inform. Process. Syst.*, 2019, pp. 4696–4705.
- [49] L. v. d. Maaten and G. Hinton, "Visualizing data using t-sne," *Journal of machine learning research*, pp. 2579–2605, 2008.
- [50] A. Paszke, S. Gross, S. Chintala, G. Chanan, E. Yang, Z. DeVito, Z. Lin, A. Desmaison, L. Antiga, and A. Lerer, "Automatic differentiation in pytorch," in *Adv. Neural Inform. Process. Syst. Worksh.*, 2017.
- [51] A. Iscen, G. Tolias, P. Gosselin, and H. Jégou, "A comparison of dense region detectors for image search and fine-grained classification," *IEEE Trans. Image Process.*, vol. 24, no. 8, pp. 2369–2381, 2015.
- [52] C. Zhang, C. Liang, L. Li, J. Liu, Q. Huang, and Q. Tian, "Fine-grained image classification via low-rank sparse coding with general and

- class-specific codebooks,” *IEEE Transactions on Neural Networks and Learning Systems*, vol. 28, no. 7, pp. 1550–1559, 2017.
- [53] Y. Zhang, X. Wei, J. Wu, J. Cai, J. Lu, V. Nguyen, and M. N. Do, “Weakly supervised fine-grained categorization with part-based image representation,” *IEEE Trans. Image Process.*, vol. 25, no. 4, pp. 1713–1725, 2016.
- [54] W. Shi, Y. Gong, X. Tao, D. Cheng, and N. Zheng, “Fine-grained image classification using modified dcnn trained by cascaded softmax and generalized large-margin losses,” *IEEE Transactions on Neural Networks and Learning Systems*, vol. 30, no. 3, pp. 683–694, 2019.
- [55] Y. Peng, X. He, and J. Zhao, “Object-part attention model for fine-grained image classification,” *IEEE Trans. Image Process.*, vol. 27, no. 3, pp. 1487–1500, 2018.
- [56] H. Zheng, J. Fu, Z. Zha, J. Luo, and T. Mei, “Learning rich part hierarchies with progressive attention networks for fine-grained image recognition,” *IEEE Trans. Image Process.*, vol. 29, pp. 476–488, 2020.
- [57] T. Lin, A. RoyChowdhury, and S. Maji, “Bilinear convolutional neural networks for fine-grained visual recognition,” *IEEE Trans. Pattern Anal. Mach. Intell.*, vol. 40, no. 6, pp. 1309–1322, 2018.
- [58] C. Zhang, C. Liang, L. Li, J. Liu, Q. Huang, and Q. Tian, “Fine-grained image classification via low-rank sparse coding with general and class-specific codebooks,” *IEEE Transactions on Neural Networks and Learning Systems*, vol. 28, no. 7, pp. 1550–1559, 2017.
- [59] W. Shi, Y. Gong, X. Tao, D. Cheng, and N. Zheng, “Fine-grained image classification using modified dcnn trained by cascaded softmax and generalized large-margin losses,” *IEEE Transactions on Neural Networks and Learning Systems*, vol. 30, no. 3, pp. 683–694, 2019.
- [60] T. Xiao, T. Xia, Y. Yang, C. Huang, and X. Wang, “Learning from massive noisy labeled data for image classification,” in *CVPR*, 2015, pp. 2691–2699.
- [61] C. Zhang, S. Bengio, M. Hardt, B. Recht, and O. Vinyals, “Understanding deep learning requires rethinking generalization,” in *Int. Conf. Learn. Represent.*, 2017.
- [62] I. J. Goodfellow, J. Shlens, and C. Szegedy, “Explaining and harnessing adversarial examples,” in *Int. Conf. Learn. Represent.*, 2015.
- [63] A. Kurakin, I. J. Goodfellow, and S. Bengio, “Adversarial machine learning at scale,” in *Int. Conf. Learn. Represent.*, 2017.
- [64] J. C. Peterson, R. M. Battleday, T. L. Griffiths, and O. Russakovsky, “Human uncertainty makes classification more robust,” in *Int. Conf. Comput. Vis.*, 2019.
- [65] J. Redmon, S. Divvala, R. Girshick, and A. Farhadi, “You only look once: Unified, real-time object detection,” in *IEEE Conf. Comput. Vis. Pattern Recog.*, 2016, pp. 779–788.
- [66] F. Fang, L. Li, H. Zhu, and J. Lim, “Combining faster r-cnn and model-driven clustering for elongated object detection,” *IEEE Trans. Image Process.*, vol. 29, pp. 2052–2065, 2020.
- [67] F. Sun, T. Kong, W. Huang, C. Tan, B. Fang, and H. Liu, “Feature pyramid reconfiguration with consistent loss for object detection,” *IEEE Trans. Image Process.*, vol. 28, no. 10, pp. 5041–5051, 2019.
- [68] S. Ren, K. He, R. Girshick, and J. Sun, “Faster r-cnn: Towards real-time object detection with region proposal networks,” *IEEE Trans. Pattern Anal. Mach. Intell.*, vol. 39, no. 6, pp. 1137–1149, 2017.
- [69] W. Liu, D. Anguelov, D. Erhan, C. Szegedy, S. Reed, C.-Y. Fu, and A. C. Berg, “Ssd: Single shot multibox detector,” in *Eur. Conf. Comput. Vis.*, 2016, pp. 21–37.
- [70] Z. Tian, C. Shen, H. Chen, and T. He, “Fcos: Fully convolutional one-stage object detection,” in *Int. Conf. Comput. Vis.*, 2019, pp. 9627–9636.
- [71] M. Everingham, L. Van Gool, C. K. Williams, J. Winn, and A. Zisserman, “The pascal visual object classes (voc) challenge,” *International journal of computer vision*, vol. 88, no. 2, pp. 303–338, 2010.
- [72] C. Guo, G. Pleiss, Y. Sun, and K. Q. Weinberger, “On calibration of modern neural networks,” in *ICML*, 2017, pp. 1321–1330.